Photon emission from quark-gluon plasma out of equilibrium

Sigtryggur Hauksson,* Sangyong Jeon, and Charles Gale
Department of Physics, McGill University, 3600 University Street, Montreal, QC, H3A 2T8, Canada

(Received 18 September 2017; published 10 January 2018)

The photon emission from a nonequilibrium quark-gluon plasma is analyzed. We derive an integral equation that describes photon production through quark-antiquark annihilation and quark bremsstrahlung. It includes coherence between different scattering sites, also known as the Landau-Pomeranchuk-Migdal effect. These leading-order processes are studied for the first time together in an out-of-equilibrium field theoretical treatment that enables the inclusion of viscous corrections to the calculation of electromagnetic emission rates. In the special case of an isotropic, viscous, plasma the integral equation only depends on three constants, which capture the nonequilibrium nature of the medium.

DOI: 10.1103/PhysRevC.97.014901

I. INTRODUCTION

Relativistic collisions of large nuclei allow the study of quantum chromodynamics (QCD): the theory of the nuclear strong interaction matter at high temperatures. Experiments performed at the Relativistic Heavy Ion Collider (RHIC) and the Large Hadron Collider (LHC) have indeed shown that such collisions create droplets of quark-gluon plasma (QGP) [1]. A significant breakthrough in the relativistic heavy-ion program has been the realization that this fluid and its evolution can be characterized by relativistic hydrodynamics, which describes long-wavelength excitations [2]. Therefore, those experiments have the potential to give access to the transport coefficients of QGP, such as shear and bulk viscosity. These coefficients are fundamental properties of QCD.

There has been extensive work on extracting the viscosity of QGP from soft hadronic observables [3]. In addition, electromagnetic observables, i.e., photons and dileptons, can play an important role in that endeavor [4,5]. They are emitted throughout the evolution of the QGP and escape from the medium unaffected by final-state interaction. This paper will focus on the production of real photons.

In order to evaluate the effects of viscosity on photons one must study their out-of-equilibrium emission. At leading order in the strong coupling constant there are two channels for photon production in QGP. First, there are two-to-two scattering channels with a photon in the final state. They were first calculated in Refs. [6,7] for thermal equilibrium. Since then there have been a number of works on these processes in an out-of-equilibrium QGP such as for finite fugacities [8–10], in an anisotropic QGP [11], for shear viscous corrections [12,13], and for bulk viscous corrections [14]. Note that consistent calculations of the electromagnetic emissivity should include non-equilibrium corrections to the thermal mass of the soft mediators.

Second, there are inelastic channels with bremsstrahlung off a quark and the pair annihilation of a quark and antiquark, see Fig. 1. These processes contribute as much to photon emission as two-to-two scattering [15]. The photon is emitted almost collinearly to the quark, which entails a large decoherence time. This means that the quarks can exchange arbitrarily many soft gluons with the medium during the formation of the photon. This leading-order complication is known as the Landau-Pomeranchuk-Migdal (LPM) effect [16–19]. It means that in addition to the diagrams in Fig. 1 one must sum up diagrams with an arbitrary number of gluon exchanges such as in Fig. 4. The LPM effect was first treated consistently in Refs. [20,21] for a medium in thermal equilibrium where it was shown to reduce photon production because of coherence between different emission sites.

This paper treats the photon production through inelastic channels in a nonequilibrium QGP for the first time, using a field theoretical derivation that includes the LPM effect without relying on the Kubo-Martin-Schwinger (KMS) [22] relation which describes detailed balance in thermal equilibrium. The field-theoretical techniques used here differ from those employed in Ref. [23], where kinetic theory was used to analyze inelastic scattering of quarks and gluons.

The paper is organized as follows. In Sec. II we review the real-time formalism and derive expressions for resummed propagators. In Sec. III we discuss the resummed rr propagator for soft gluons and show that the LPM effect is leading order in nonequilibrium systems. Section IV discusses the resummed occupation number of hard quarks. In Sec. V we sum up the different diagrams contributing to the LPM effect and derive an integral equation describing the inelastic channels. Finally, we conclude in Sec. VI and indicate future directions. We will use the $(+,-,-,-)$ metric. If P^μ is a four-vector we write $P^\mu = (p^0, \mathbf{p})$ and define $p = |\mathbf{p}|$ and $\hat{\mathbf{p}} = \mathbf{p}/p$.

II. RESUMMED PROPAGATORS IN THE REAL-TIME FORMALISM

Out-of-equilibrium quantum field theory is best described in the real-time formalism where a closed time contour leads to the doubling of degrees of freedom [24,25]. In this paper we

*Corresponding author: sigtryggur.hauksson@mail.mcgill.ca

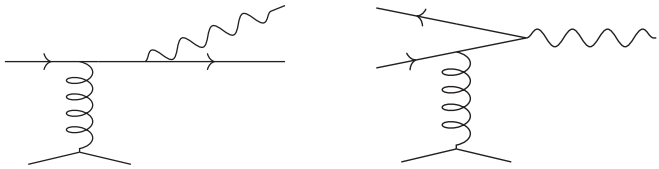

FIG. 1. Photon production through quark bremsstrahlung and the annihilation of a quark and an antiquark. For the first process, the diagram with the photon emitted left of the vertex is included but not shown, as is that with the gluon connecting to the antiquark in the second process.

mostly work in the r/a basis [26], which is defined by

$$\phi_r = \tfrac{1}{2}(\phi_1 + \phi_2), \quad \phi_a = \phi_1 - \phi_2. \tag{1}$$

The propagators are

$$D_{cd}(x,y) = \langle \phi_c(x)\phi_d^\dagger(y)\rangle = \mathrm{Tr}[\rho_0\, \mathcal{T}_C \phi_c(x)\phi_d^\dagger(y)], \tag{2}$$

where c and d are either r or a. The initial density matrix ρ_0 determines the out-of-equilibrium evolution of the system. In the r/a basis, vertices have an odd number of a indices, see Fig. 2. This basis has numerous advantages: The aa propagator vanishes identically and the bare ra and ar propagators only include vacuum contributions. Furthermore it allows for easier power counting. For concreteness we consider complex scalar fields in this section but our arguments can easily be generalized.

In this paper we study translationally invariant systems. In other words, our calculation is for a homogeneous and static brick of out-of-equilibrium QGP. This approximation is justified when the mean-free path of quasiparticles is much smaller scale than the macroscopic scale at which hydrodynamical quantities change appreciably. In a translationally invariant system the propagators are

$$\begin{aligned} D_{rr}(x) &= \tfrac{1}{2}\langle\{\phi(x),\phi^\dagger(0)\}\rangle \\ D_{ra}(x) &= \theta(x^0)\langle[\phi(x),\phi^\dagger(0)]\rangle \\ D_{ar}(x) &= -\theta(-x^0)\langle[\phi(x),\phi^\dagger(0)]\rangle \\ D_{aa}(x) &= 0. \end{aligned} \tag{3}$$

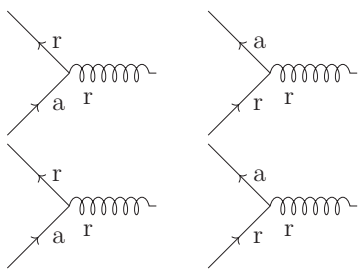

FIG. 2. Quark-gluon vertices in the r/a basis in the real-time formalism.

We see that $D_{ra} = D_{\mathrm{ret}}$ and $D_{ar} = D_{\mathrm{adv}}$. Going to momentum space with momentum P

$$\begin{aligned} D_{\mathrm{ret}}(P)^* &= \int d^4x\; e^{-iP\cdot x}\theta(x^0)\langle[\phi(0),\phi^\dagger(x)]\rangle \\ &= \int d^4x\; e^{iP\cdot x}\theta(-x^0)\langle[\phi(0),\phi^\dagger(-x)]\rangle \\ &= \int d^4x\; e^{iP\cdot x}\theta(-x^0)\langle[\phi(x),\phi^\dagger(0)]\rangle \\ &= -D_{\mathrm{adv}}(P), \end{aligned} \tag{4}$$

where we did a change of variables $x \to -x$ in the second line and then used translational invariance. This shows that the resummed propagators only have two independent components. The bare retarded propagator can easily be evaluated because the commutator of free bosonic fields is just a number so summing over all states is trivial. It is the same as in vacuum,

$$D^0_{\mathrm{ret}}(P) = \frac{i}{P^2 + i\epsilon p^0}. \tag{5}$$

We have yet to find the rr propagator. In thermal equilibrium the Kubo-Martin-Schwinger (KMS) relation stipulates that

$$D_{rr}(P) = \big(\tfrac{1}{2} + f_B(p^0)\big)[D_{\mathrm{ret}}(P) - D_{\mathrm{adv}}(P)] \tag{6}$$

so there is only one independent propagator. Here $f_B(p^0)$ is the Bose-Einstein distribution [24]. This expression is valid at every order in perturbation theory and thus offers great simplification. Using Eq. (5) the bare rr propagator is

$$D^0_{rr}(P) = \big(\tfrac{1}{2} + f_B(p)\big)2\pi\delta(P^2). \tag{7}$$

In nonequilibrium systems one cannot obtain a general expression for the resummed rr propagator. In analogy with the equilibrium case the bare propagator is

$$D^0_{rr}(P) = \big(\tfrac{1}{2} + \theta(p^0)f(\mathbf{p}) + \theta(-p^0)f(-\mathbf{p})\big)2\pi\delta(P^2), \tag{8}$$

where the ansatz, $f(\mathbf{p})$, is a general momentum distribution characterizing the system. For mirror symmetric momentum distributions, $f(\mathbf{p}) = f(-\mathbf{p})$, the bracket reduces to $1/2 + f(\mathbf{p})$, see Ref. [27] for a discussion. Equation (8) can be justified from first principles as in Refs. [28,29]. Assuming an initial density matrix ρ_0, one Legendre-transforms the path integral from external sources to connected n-point functions. This gives rise to an infinite tower of equations corresponding to the BBGKY hierarchy in kinetic theory. Truncating the tower at second order and assuming that propagators vary slowly in space one gets Eq. (8) at lowest order in the coupling. The function f can be shown to be real and positive and the equations of motion reduce to a Boltzmann equation for f. Therefore, at leading order in the coupling constant it should be interpreted as a momentum distribution of particles. The δ function shows that the quasiparticles are on shell to lowest order. In this approach f is left unspecified and can be chosen to match a hydrodynamical evolution of the QGP.

Demanding that propagators vary slowly in time sets constraints on how far from equilibrium one can go. In anisotropic and translationally invariant systems the retarded gluon propagator acquires a pole with $\mathrm{Im}\,\omega > 0$ [30]. This pole signals the exponential growth of the occupation density of soft gluons

[31], which can invalidate our assumption of translational invariance. Specifically, the pole introduces divergences in momentum integrals over G_{rr} for soft gluons. Throughout our analysis we will assume that the anisotropy is small enough so that this divergence does not appear at leading order in the coupling. As an example consider a momentum distribution of the form [30]

$$f(\mathbf{p}) = f_{\rm eq}(\sqrt{p^2 + \xi(\mathbf{n}\cdot\mathbf{p})^2}), \tag{9}$$

where $f_{\rm eq}$ is an equilibrium distribution and $\mathbf{n}$ is a unit vector specifying the direction of the anisotropy ξ (in general $-1 \leqslant \xi < \infty$). We will show below that we must demand $|\xi| \lesssim g^2$ if the divergence is to be subleading. On the contrary, isotropic systems can be much farther away from equilibrium without our analysis breaking down. In summary, we study systems with low anisotropy that are close enough to local thermal equilibrium so that the equilibrium power counting scheme is unaltered. This guarantees that the hard thermal loop (HTL) scheme remains valid.

In this paper we will need resummed propagators in out-of-equilibrium systems. For the convenience of the reader we reproduce some known results for scalar field theory in the real-time formalism, see Ref. [32]. The Dyson equation is

$$\begin{bmatrix} D_{rr} & D_{ra} \\ D_{ar} & D_{aa} \end{bmatrix} = \begin{bmatrix} D^0_{rr} & D^0_{ra} \\ D^0_{ar} & D^0_{aa} \end{bmatrix} + \begin{bmatrix} D^0_{rr} & D^0_{ra} \\ D^0_{ar} & D^0_{aa} \end{bmatrix}(-i) \times \begin{bmatrix} \Pi_{rr} & \Pi_{ra} \\ \Pi_{ar} & \Pi_{aa} \end{bmatrix}\begin{bmatrix} D_{rr} & D_{ra} \\ D_{ar} & D_{aa} \end{bmatrix}. \tag{10}$$

where, say, Π_{aa} is the self-energy sourced by two a fields. Using $D_{aa} = D^0_{aa} = 0$ one finds that $\Pi_{rr} = 0$. Defining $\Pi_{ar} = \Pi_{\rm ret}$ one obtains

$$D_{\rm ret} = D^0_{\rm ret} + D^0_{\rm ret}(-i\Pi_{\rm ret})D_{\rm ret}, \tag{11}$$

which gives

$$D_{\rm ret} = \frac{i}{P^2 - \Pi_{\rm ret}}. \tag{12}$$

This equation gives the dispersion relation for the quasiparticles, i.e., their thermal mass and decay width. Similarly

$$D_{\rm adv} = \frac{i}{P^2 - \Pi_{\rm adv}}, \tag{13}$$

where $\Pi_{\rm adv} = \Pi_{ra} = \Pi^*_{\rm ret}$ in translationally invariant systems.

The Dyson equation for D_{rr} is more complicated. Defining $D_< = D_{12}$ and $D_> = D_{21}$ we can write

$$D_{rr} = \tfrac{1}{2}(D_> + D_<) = D_< + \tfrac{1}{2}(D_{\rm ret} - D_{\rm adv}) \tag{14}$$

since $D_> - D_< = D_{\rm ret} - D_{\rm adv}$. We will analyze $D_<$ to obtain equations with a clear physical interpretation. Using the rr component of Eq. (10), Eq. (11), and the corresponding equation for $D_{\rm adv}$ one gets

$$D_< = D^0_< + D^0_{\rm ret}(-i\Pi_{\rm ret})D_< + D^0_<(-i\Pi_{\rm adv})D_{\rm adv} + D^0_{\rm ret}(-i\Pi_<)D_{\rm adv}, \tag{15}$$

where

$$\Pi_< = \Pi_{aa} - \tfrac{1}{2}\Pi_{\rm ret} + \tfrac{1}{2}\Pi_{\rm adv}, \tag{16}$$

In the original 12 basis $\Pi_< = -\Pi_{12}$ in our convention. This component of the self-energy describes the creation rate of quasiparticles [24]. Solving for $D_<$ using Eq. (12) one gets

$$D_< = \frac{\left(-iD^0_{\rm ret}\right)^{-1} D^0_< \left(-iD^0_{\rm adv}\right)^{-1} + i\Pi_<}{\left[\left(-iD^0_{\rm ret}\right)^{-1} - \Pi_{\rm ret}\right]\left[\left(-iD^0_{\rm adv}\right)^{-1} - \Pi_{\rm adv}\right]}. \tag{17}$$

For nonvanishing self-energy the first term is zero because

$$D^0_<\left(D^0_{\rm ret}\right)^{-1} \propto P^2\delta(P^2) = 0. \tag{18}$$

This is true since our theory is defined in momentum space and assumes translational invariance. Thus

$$D_< = D_{\rm ret}(-i\Pi_<)D_{\rm adv} \tag{19}$$

and

$$D_{rr} = \tfrac{1}{2}(D_{\rm ret} - D_{\rm adv}) + D_{\rm ret}(-i\Pi_<)D_{\rm adv}. \tag{20}$$

In deriving this equation we never had to invert the order of propagators. Thus it is equally valid for spinors and spin-1 bosons whose propagators are matrices in the space-time indices.

For $D_> = D_{21}$ one similarly gets that

$$D_> = D_{\rm ret}(-i\Pi_>)D_{\rm adv}, \tag{21}$$

where $\Pi_> = -\Pi_{21}$ describes the annihilation of quasiparticles. It is easy to see that

$$\Pi_{\rm ret} - \Pi_{\rm adv} = \Pi_> - \Pi_<, \tag{22}$$

which reduces to

$$2i\,{\rm Im}\,\Pi_{\rm ret} = \Pi_> - \Pi_< \tag{23}$$

in translationally invariant systems. This last equation says that the decay width of a quasiparticle is the difference of the annihilation and creation rate.

For scalar particles we can go further and derive a more intuitive expression for D_{rr}. In translationally invariant systems Eq. (12) and (13) give that

$$D_{\rm ret} - D_{\rm adv} = 2({\rm Im}\,\Pi_{\rm ret})D_{\rm ret}D_{\rm adv}. \tag{24}$$

Thus we see that

$$D_{rr} = \left[\frac{1}{2} + \frac{\Pi_<}{2i\,{\rm Im}\,\Pi_{\rm ret}}\right](D_{\rm ret} - D_{\rm adv}). \tag{25}$$

This equation has a striking resemblance with the rr propagator in equilibrium, Eq. (6). Indeed $\Pi_</2i\,{\rm Im}\,\Pi_{\rm ret}$ reduces to the Bose-Einstein distribution by using the KMS relation for self-energies. In nonequilibrium systems $\Pi_</2i\,{\rm Im}\,\Pi_{\rm ret}$ is in general not the same as the bare momentum distribution $f(\mathbf{p})$. It can be viewed as a resummed occupation density. We emphasize that we have only derived Eq. (25) for scalar particles since we needed to invert the order of propagators. In the next two sections we will derive a similar relation for soft gluons and hard quarks and evaluate the resummed occupation density explicitly.

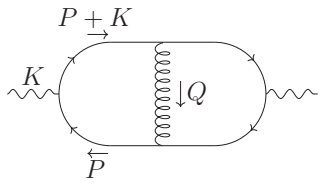

FIG. 3. Definition of momenta in the argument for bremsstrahlung and pair annihilation contribution at leading order.

III. *rr* PROPAGATOR OF SOFT GLUONS

The photon production rate is given by the 12 component of the photon polarization tensor

$$k\frac{dR}{d^3k} = \frac{i}{2(2\pi)^3}\left(\Pi_{12}^{\gamma}\right)_{\mu}^{\mu}, \tag{26}$$

where $\mathbf{k}$ is the photon momentum and Π_{12}^{γ} is one component of the photon polarization tensor. This equation is valid in nonequilibrium systems as has been shown in Ref. [33].

The diagram corresponding to bremsstrahlung and quark-antiquark pair annihilation is in Fig. 3. Due to the LPM effect the quarks can have arbitrarily many gluon exchanges, see Fig. 4. We will now briefly explain why these diagrams contribute at leading order for a medium in thermal equilibrium, see Refs. [20,34] for further details. The quarks are hard, $P \sim T$, and nearly on shell, $P^2 \sim g^2T^2$, where T is the temperature and $g \ll 1$ is the strong coupling constant. The photon is emitted with an angle $\theta \sim g$ relative to the quark momentum. Finally, the exchanged gluons are soft, $Q \sim gT$, forcing us to use resummed propagators.

We analyze the diagram in Fig. 3. In thermal equilibrium the rr propagator for soft gluons is

$$G_{rr}(Q) = \left(\frac{1}{2} + f_B(q^0)\right)[G_{\text{ret}} - G_{\text{adv}}] \sim \frac{1}{g^3T^2}, \tag{27}$$

where $f_B(q^0) \sim T/q^0 \sim 1/g$ and the retarded gluon propagator is $G_{\text{ret}} \sim 1/g^2T^2$. Furthermore, each pair of quark propagators gives pinching poles of order $1/g^2$. This can be seen more easily for bare scalars for which

$$\begin{aligned}&\int dp^0\ D_{ar}(K+P)D_{ra}(P)\\ &= \int dp^0\ \frac{1}{[(p^0+i\epsilon)^2 - p^2][(p^0+k-i\epsilon)^2 - |\mathbf{p}+\mathbf{k}|^2]}\\ &\sim \frac{1}{T^2} \times \frac{1}{p+k-|\mathbf{p}+\mathbf{k}|} \sim \frac{1}{g^2T^3},\end{aligned} \tag{28}$$

where we did a contour integration and used that $\hat{\mathbf{p}}\cdot\hat{\mathbf{k}} = 1 - O(g^2)$. In real calculations one must use resummed fermion propagators since their self-energy is $O(g^2)$. Finally each gluon vertex contributes a factor g and each photon vertex contributes a factor e as well as a factor g because of kinematics [20]. Including a g^3 phase space suppression because $\mathbf{q}$ is soft and a g^2 suppression because $\mathbf{p}$ is collinear with $\mathbf{k}$ one sees that the diagram is of order g^2e^2. A similar analysis shows that Fig. 4 is also leading order.

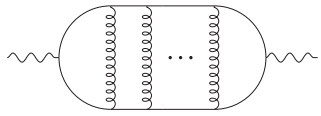

FIG. 4. The diagrams for the LPM effect.

The above argument relied mostly on kinematics and is therefore equally valid in nonequilibrium systems.[1] Nevertheless, it assumed thermal equilibrium in two crucial places. First, the authors of Ref. [20] used a KMS condition for four-point functions to show that only S_{ra} and S_{ar} contribute to the pinching poles. We provide a more general argument in the next two sections. Second, Eq. (27) for the rr propagator was derived using the KMS condition.

In general the retarded self-energy for soft gluons is [23,35]

$$\begin{aligned}\Pi_{\text{ret}}^{\mu\nu}(Q) = -2g^2 \int \frac{d^3p}{(2\pi)^3}\frac{1}{2p}\left(\frac{\partial f_{\text{tot}}(\mathbf{p})}{\partial P^{\omega}}\right)\\ \times\left[-P^{\mu}g^{\omega\nu} + \frac{Q^{\omega}P^{\mu}P^{\nu}}{P\cdot Q + i\epsilon}\right],\end{aligned} \tag{29}$$

where

$$f_{\text{tot}} = N_f f_q + N_f f_{\bar{q}} + 2N_c f_g \tag{30}$$

with f_q, $f_{\bar{q}}$, f_g the distribution for quarks, antiquarks, and gluons respectively. We should interpret $\partial f_{\text{tot}}(\mathbf{p})/\partial p^0 = 0$. The 12 component, $\Pi_<(Q)$, has also been evaluated for spacelike gluons [23]. It is

$$\begin{aligned}\Pi_<^{\mu\nu}(Q) = -ig^2 \int \frac{d^3p}{(2\pi)^3}\frac{P^{\mu}P^{\nu}}{p}2\pi\delta(P\cdot Q)\Big|_{p^0=p}\\ \times [N_f f_q(\mathbf{p})[1-f_q(\mathbf{p})] + N_f f_{\bar{q}}(\mathbf{p})[1-f_{\bar{q}}(\mathbf{p})]\\ + 2N_c f_g(\mathbf{p})[1+f_g(\mathbf{p})]].\end{aligned} \tag{31}$$

In both expressions we have used that $P \gg Q$. Equation (31) has an intuitive interpretation. The soft gluons are sourced by hard quarks and gluons with momentum P. The factor $f_q(\mathbf{p})[1-f_q(\mathbf{p})]$ is the density of the incoming and outgoing hard quark including Pauli blocking. Similarly $f_g(\mathbf{p})[1+f_g(\mathbf{p})]$ describes the hard gluon. These expressions are true as long as the hard thermal loop (HTL) scheme is valid. This puts some mild constraints on the momentum distribution [23], such as that the density of soft gluons cannot be exceedingly high.

We can now see that $G_{rr} \sim g^{-3}$ for soft gluons in nonequilibrium systems. Clearly $\Pi_{\text{ret}} \sim g^2T^2$ so $G_{\text{ret}} \sim g^{-2}$ while $\Pi_< \sim gT^2$ because of the δ function in Eq. (31). Thus, using Eq. (20),

$$G_{rr} \approx G_{\text{ret}}(-i\Pi_<)G_{\text{adv}} \sim \frac{1}{g^3}, \tag{32}$$

which ensures that the LPM effect matters at leading order.

[1] In systems that are far away from thermal equilibrium there is no well-defined temperature. Then the scale T should be replaced by the hard scale, which contributes to the greatest number of particles, see Ref. [23] for further details.

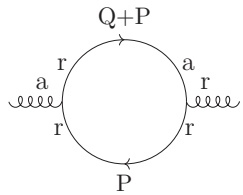

FIG. 5. One of the diagrams contributing to $\Pi_{\rm ret} = \Pi_{ar}$.

At first sight it might be surprising that $\Pi_<$ and $\Pi_{\rm ret}$ differ by a power of g since they come from the same Feynman diagrams. The reason for the difference is the following: The vertices give factors $P^\mu P^\nu$, which are $O(1)$ and factors $P^\mu Q^\nu + Q^\mu P^\nu$ and $P\cdot Q\, g^{\mu\nu}$, which are $O(g)$. For the retarded self-energy all terms with $P^\mu P^\nu$ cancel giving a suppression in g. As an example we can look at Fig. 5. The diagram goes like

$$\begin{aligned}&\int d^4P\,\frac{P^\mu P^\nu \delta(P^2)}{(Q+P)^2+i\epsilon(q^0+p^0)}\\ &\sim \int d^3p\,\frac{P^\mu P^\nu}{2q^0p^0-2\mathbf{p}\cdot\mathbf{q}+i\epsilon p^0}\bigg|_{p^0=p}\\ &\quad+\int d^3p\,\frac{P^\mu P^\nu}{2q^0p^0-2\mathbf{p}\cdot\mathbf{q}+i\epsilon p^0}\bigg|_{p^0=-p}\end{aligned}\tag{33}$$

at leading order. The two terms cancel as can be seen by doing $\mathbf{p}\to-\mathbf{p}$ in the last integral. Such a cancellation does not take place when the vertex factor is $P^\mu Q^\nu + Q^\mu P^\nu$ or $P\cdot Q\, g^{\mu\nu}$.

The gluon rr propagator is more complicated in a nonequilibrium plasma than in equilibrium. In particular it has an imaginary part. Using the definition

$$G^{\mu\nu}_{rr}(P) = \frac{1}{2}\int d^4x\; e^{iP\cdot x}\langle\{A^\mu(x),A^\nu(0)\}\rangle\tag{34}$$

we get that $G^{\mu\nu}_{rr}(P)^* = G^{\mu\nu}_{rr}(-P)$. In translationally invariant systems we furthermore get that

$$\begin{aligned}G^{\mu\nu}_{rr}(P) &= \frac{1}{2}\int d^4x\; e^{-iP\cdot x}\langle\{A^\mu(-x),A^\nu(0)\}\rangle\\ &= \frac{1}{2}\int d^4x\; e^{-iP\cdot x}\langle\{A^\nu(x),A^\mu(0)\}\rangle\\ &= G^{\nu\mu}_{rr}(-P),\end{aligned}\tag{35}$$

where we did a change of variables $x\to -x$ in the first line and translated the propagator in the second line. These results are clearer when writing

$$G^{\mu\nu}_{rr}(P) = \mathrm{Re}\, G^{\mu\nu}_{rr}(P) + i\,\mathrm{Im}\, G^{\mu\nu}_{rr}(P).\tag{36}$$

Then $\mathrm{Re}\, G^{\mu\nu}_{rr}(-P) = \mathrm{Re}\, G^{\mu\nu}_{rr}(P)$ and $\mathrm{Im}\, G^{\mu\nu}_{rr}(-P) = -\mathrm{Im}\, G^{\mu\nu}_{rr}(P)$. Furthermore, Eq.(35) shows that $\mathrm{Re}\, G_{rr}$ is symmetric and $\mathrm{Im}\, G_{rr}$ is antisymmetric under the interchange of the space-time indices. Evaluation of G_{rr} explicitly given some momentum distribution function f is a subject for future research. The 00 component has been evaluated using an anisotropic momentum distribution as it has applications to the heavy-quark potential in QGP [36].

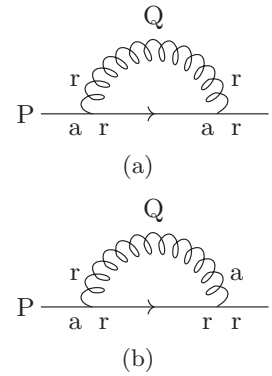

FIG. 6. Diagrams contributing to $\Sigma_{\rm ret}$ at leading order in g.

The imaginary part of G_{rr} might seem surprising. It is helpful to consider how it comes about. We can always write

$$G_{rr} = G_{\rm ret}\frac{-i(\Pi_> + \Pi_<)}{2}G_{\rm adv},\tag{37}$$

where

$$\big[1 - G^0_{\rm ret}(-i\Pi_{\rm ret})\big]G_{\rm ret} = G^0_{\rm ret}\tag{38}$$

and similarly for $G_{\rm adv}$. The bare propagator and the HTL self-energy is symmetric in the space-time indices so the same goes for $G_{\rm ret}$ and $G_{\rm adv}$. Thus G_{rr} is the product of three symmetric matrices. In general

$$G^T_{rr} = G_{\rm adv}\frac{-i(\Pi_> + \Pi_<)}{2}G_{\rm ret}\tag{39}$$

will be different from G_{rr} because these matrices do not commute. In equilibrium (and for any isotropic momentum distribution) the only available tensors are $g^{\mu\nu}$, the external momentum P^μ, and the plasma four-velocity, u^μ. Therefore all matrices are spanned by $g^{\mu\nu}$, $P^\mu P^\nu$, and the projection operators P_T and P_L [37]. These four matrices commute so $G^T_{rr} = G_{rr}$ and G_{rr} is real. In an anisotropic plasma there are additional tensors describing the anisotropy and therefore more matrices. They will not all commute in general giving G_{rr} an imaginary part.

IV. OCCUPATION DENSITY OF HARD QUARKS

To evaluate the LPM effect we need the rr propagator for hard and nearly on-shell quarks, i.e., $S_{rr}(P)$ with $P\sim T$ and $P^2\sim g^2T^2$. We will show that at leading order

$$S_{rr} = \big[\tfrac{1}{2} - F\big](S_{\rm ret} - S_{\rm adv}),\tag{40}$$

just as for scalars. Here $F(P) := -P\cdot\Sigma_</2iP\cdot\mathrm{Im}\,\Sigma_{\rm ret}$ is a resummed occupation density.

We begin by evaluating $\Sigma_{\rm ret}$. The contributing diagrams can be seen in Fig. 6. For an internal particle with soft momentum, $O(gT)$, we must use a HTL resummed propagator, while for hard particles we use bare propagators. There are a few different momentum regimes. When the loop momentum is hard, $Q\sim T$, the two diagrams give rise to the thermal

mass

$$m_\infty^2 = 2P\cdot \mathrm{Re}\,\Sigma_{\mathrm{ret}}(P) = 2g^2C_F\int\frac{d^3p}{(2\pi)^3}\,\frac{2f_g(\mathbf{p})+f_q(\mathbf{p})+f_{\bar q}(\mathbf{p})}{2p}. \quad (41)$$

The contribution of this momentum regime to $\mathrm{Im}\,\Sigma_{\mathrm{ret}}$ is phase space suppressed because both G^0_{rr} and $\mathrm{Im}\,S^0_{\mathrm{ret}}$ contain a δ function forcing the internal particles to be on shell.[2]

We now focus on the top diagram in Fig. 6, which is given by

$$\Sigma_{\mathrm{ret}}(P)|_{(a)} = -ig^2C_F\int\frac{d^4Q}{(2\pi)^4}\,G^{\mu\nu}_{rr}(Q)\,\gamma_\mu S_{\mathrm{ret}}(P-Q)\gamma_\nu. \quad (42)$$

When the gluon is soft and the quark is hard the leading-order contribution is

$$\Sigma_{\mathrm{ret}}(P)|_{\mathrm{soft}} = g^2C_F\int\frac{d^4Q}{(2\pi)^4}\,\gamma_\mu \not{P}\gamma_\nu\,G^{\mu\nu}_{rr}(Q) \times\left[-i\pi\,\mathrm{sgn}(p^0)\,\delta(2P\cdot Q)+\frac{1}{-2P\cdot Q}\right], \quad (43)$$

where we have substituted the bare quark propagator. We have used that the quark is on-shell, $P^2\sim g^2T^2$. Using the properties of $G^{\mu\nu}_{rr}(Q)$ under the interchange of the space-time indices and under $Q\to -Q$ we can write

$$\Sigma_{\mathrm{ret}}(P)|_{\mathrm{soft}} = \mathrm{Re}\,\Sigma^{\mathrm{p}}_\mu\,\gamma^5\gamma^\mu + i\,\mathrm{Im}\,\Sigma_\mu\,\gamma^\mu, \quad (44)$$

where

$$\mathrm{Im}\,\Sigma_\omega = -g^2C_F\int^{gT}\frac{d^4Q}{(2\pi)^4}\,(P_\mu g_{\nu\omega}+P_\nu g_{\mu\omega}-g_{\mu\nu}P_\omega) \times\pi\,\mathrm{sgn}(p^0)\,\delta(2P\cdot Q)\,\mathrm{Re}\,G^{\mu\nu}_{rr} \quad (45)$$

and we have a pseudovector component

$$\mathrm{Re}\,\Sigma^{\mathrm{p}}_\omega = g^2C_F\,\varepsilon_{\omega\rho\mu\nu}P^\rho\int^{gT}\frac{d^4Q}{(2\pi)^4}\,\frac{\mathrm{Im}\,G^{\mu\nu}_{rr}}{2P\cdot Q}. \quad (46)$$

Here we used the identity [38]

$$\gamma_\mu\gamma_\rho\gamma_\nu = g_{\mu\rho}\gamma_\nu+g_{\rho\nu}\gamma_\mu-g_{\mu\nu}\gamma_\rho+i\epsilon_{\sigma\mu\rho\nu}\gamma^\sigma\gamma^5 \quad (47)$$

to separate the symmetrical and antisymmetrical part of G_{rr}. The expression in Eq. (44) is clearly leading order because $G_{rr}\sim g^{-3}T^2$ and $Q\sim gT$. The vector term with $\mathrm{Im}\,\Sigma_\mu$ is both present in equilibrium and nonequilibrium plasma. It determines the decay width of hard quarks, Γ, through

$$-\frac{1}{2}p^0\Gamma = P\cdot\mathrm{Im}\,\Sigma_{\mathrm{ret}} = -2\pi g^2C_F\,\mathrm{sgn}(p^0) \times P_\mu P_\nu\int^{gT}\frac{d^4Q}{(2\pi)^4}\,\mathrm{Re}\,G^{\mu\nu}_{rr}(Q)\,\delta(2P\cdot Q). \quad (48)$$

[2]In our notation Σ_{ret} can denote both a spinor matrix and a four-vector, i.e., $\Sigma_{\mathrm{ret}}=\Sigma^\mu_{\mathrm{ret}}\gamma_\mu$.

The pseudovector term with $\mathrm{Re}\,\Sigma^p_\mu$ is only present in anisotropic systems because it includes the imaginary part of G_{rr}.

There are no further leading-order contributions to Σ_{ret}. The case of a soft internal quark, $P-Q\sim gT$, in Fig. 6(a) is subleading because there is no enhancement from soft gluons. Similarly, Fig. 6(b) is subleading when either particle is soft because the g^{-3} contribution from G_{rr} is missing.

We can now derive the retarded quark propagator. We have shown that the full self-energy is

$$\Sigma_{\mathrm{ret}} = \Sigma_\mu\,\gamma^\mu + \mathrm{Re}\,\Sigma^{\mathrm{p}}_\mu\,\gamma^5\gamma^\mu, \quad (49)$$

where $\mathrm{Re}\,\Sigma_\mu$ gives the thermal mass in Eq. (41) and $\mathrm{Im}\,\Sigma_\mu$ and $\mathrm{Re}\,\Sigma^{\mathrm{p}}_\mu$ are as before. The retarded propagator in the Dirac representation is then

$$S_{\mathrm{ret}} = \begin{bmatrix} 0 & \frac{i(P-\Sigma+\mathrm{Re}\,\Sigma^{\mathrm{p}})\cdot\sigma}{(P-\Sigma+\mathrm{Re}\,\Sigma^{\mathrm{p}})^2} \\ \frac{i(P-\Sigma-\mathrm{Re}\,\Sigma^{\mathrm{p}})\cdot\bar\sigma}{(P-\Sigma-\mathrm{Re}\,\Sigma^{\mathrm{p}})^2} & 0 \end{bmatrix}. \quad (50)$$

Because of the γ^5 matrix the pseudovector part of the self-energy, $\mathrm{Re}\,\Sigma^{\mathrm{p}}$, has different signs for positive and negative helicities. However, both helicities have the same thermal mass since $P\cdot\mathrm{Re}\,\Sigma^p_{\mathrm{ret}}$ vanishes because of the Levi-Civita tensor. The imaginary part of the self energy still has the same sign for both helicities. Thus we can write

$$S_{\mathrm{ret}} = \frac{i\not{P}}{P^2-m_\infty^2+i\Gamma p^0} \quad (51)$$

at leading order where m_∞^2 is given by Eq. (41). We have used that $(P-\Sigma)^2\approx P^2-2P\cdot\Sigma$. We see that the pseudovector component, and therefore $\mathrm{Im}\,G_{rr}$, does not contribute when considering on-shell particles, which simplifies the calculations considerably.

We can finally derive S_{rr} in Eq. (40). A similar argument as for Σ_{ret} shows that

$$P\cdot\Sigma_<(P) = 4\pi i g^2C_F[f_q(\mathbf{p})\theta(p^0)+(f_{\bar q}(-\mathbf{p})-1)\theta(-p^0)] \times P_\mu P_\nu\int^{gT}\frac{d^4Q}{(2\pi)^4}\,\mathrm{Re}\,G^{\mu\nu}_{rr}(Q)\,\delta(2P\cdot Q). \quad (52)$$

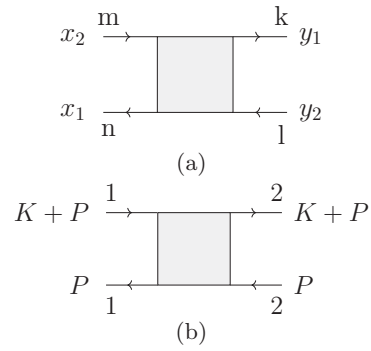

FIG. 7. Definition of the four-point function $S_{nmkl}(x_1,x_2;y_1,y_2)$ in position space. n,m,k,l are either 1 or 2. Also shown is the diagram we need to evaluate, i.e., S_{1122} in momentum space.

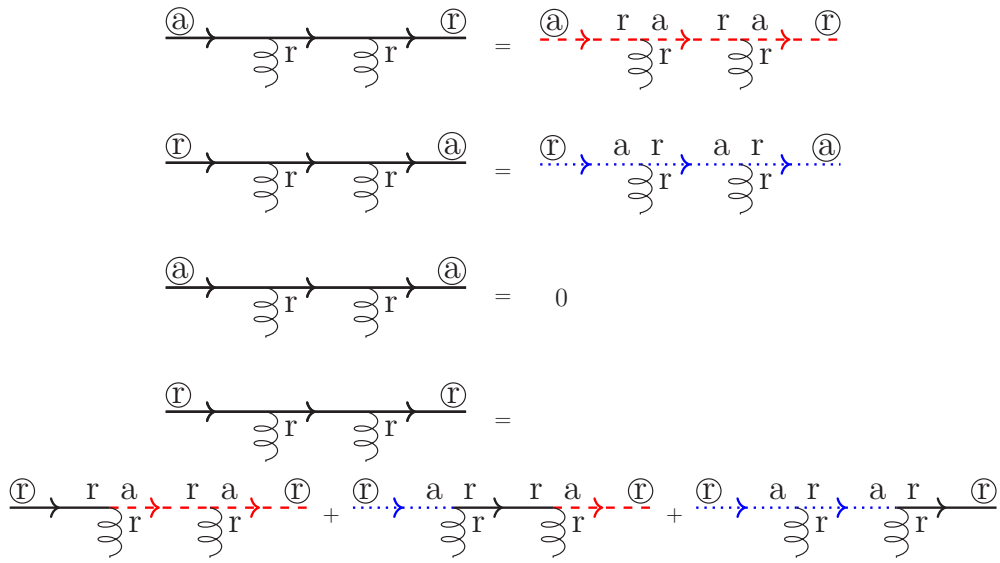

FIG. 8. Analysis of quark rails in the r/a basis.

The quark momentum distribution comes from S^0_{12} and we have used that $G_{12} \approx G_{rr}$ for soft gluons. Since

$$\not{P}\,\not{\Sigma}_<\not{P} = -P^2\,\not{\Sigma}_< + 2P\cdot\Sigma_<\not{P} \approx 2P\cdot\Sigma_<\not{P} \tag{53}$$

one can easily show that at leading order

$$\begin{aligned} S_{rr}(P) &= \tfrac{1}{2}(S_{\rm ret} - S_{\rm adv}) + S_{\rm ret}(-i\Sigma_<)S_{\rm adv} \\ &\approx \big(\tfrac{1}{2} - F(P)\big)(S_{\rm ret} - S_{\rm adv}), \end{aligned} \tag{54}$$

where

$$\begin{aligned} F(P) &:= -\frac{P\cdot\Sigma_<}{2iP\cdot{\rm Im}\,\Sigma_{\rm ret}} \\ &= f_q(\mathbf{p})\,\theta(p^0) + (1 - f_{\bar q}(-\mathbf{p}))\,\theta(-p^0). \end{aligned} \tag{55}$$

All dependence on G_{rr} cancels out in F.

Comparing with the expression for S_{rr} in equilibrium we see that F should be interpreted as a resummed occupation density. Its form makes perfect sense. In the Boltzmann equation incoming particles have $p^0 > 0$ and outgoing particles have $p^0 < 0$. Thus F is just the bare momentum distribution with Pauli blocking for outgoing quarks. This function reduces to the Fermi-Dirac distribution $f_F(p^0)$ in equilibrium as can be seen by using $1 - f_F(-x) = f_F(x)$ and noting that when going from equilibrium to nonequilibrium systems one makes the identification $f_F(|p^0|) \leftrightarrow f_q(\mathbf{p})$.

V. LPM EFFECT IN A NONEQUILIBRIUM PLASMA

We now have all the ingredients to evaluate the LPM effect in an out-of-equilibrium quark-gluon plasma, and to compute the photon production rate in Eq. (26). The photon sources are

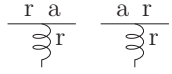

FIG. 9. Vertices that contribute at leading order.

connected to a quark and an antiquark so we need to evaluate the four-point function

$$S_{1122}(x_1,x_2;y_1,y_2) = \langle T_{\mathcal C}\{\overline{\psi}_1(x_1)\psi_1(x_2)\overline{\psi}_2(y_1)\psi_2(y_2)\}\rangle. \tag{56}$$

See Fig. 7, top diagram, for the corresponding contribution. When going to momentum space we can approximate the momentum in the quark or the antiquark rail as constant because it only changes through the exchange of soft gluons. The relevant diagram is the bottom one in Fig. 7 where K is the photon momentum and P is the loop momentum.

A. Summing four-point functions without the KMS condition

Up until now our analysis has been in the r/a basis, which enables power counting of the complicated diagrams. We must evaluate S_{1122} using the expression

$$\begin{aligned} S_{1122} = {} & S_{rrrr} + \tfrac{1}{2}(S_{arrr} + S_{rarr} - S_{rrar} - S_{rrra}) \\ & + \tfrac{1}{4}(S_{aarr} - S_{arar} - S_{arra} - S_{raar} - S_{rara} + S_{rraa}) \\ & + \tfrac{1}{8}\big(S_{raaa} + S_{araa} - S_{aara} - S_{aaar} + \tfrac{1}{2}S_{aaaa}\big). \end{aligned} \tag{57}$$

This task might look overwhelming. Each four-point function on the right-hand side is a sum of infinitely many diagrams with a different number of gluon rungs. They need not have any clear pattern in their r/a indices.

In thermal equilibrium the four-point functions have been related using the KMS condition [39]. Specifically,

$$\begin{aligned} S_{1122} = {} & \alpha_1 S_{aarr} + \alpha_2 S_{aaar} + \alpha_3 S_{aara} + \alpha_4 S_{araa} \\ & + \alpha_5 S_{raaa} + \alpha_6 S_{arra} + \alpha_7 S_{arar} + \text{c.c.}, \end{aligned} \tag{58}$$

where the coefficients depend on the Fermi-Dirac distribution. As an example $\alpha_1 = f_F(p^0 + k^0)[1 - f_F(p^0)]$. One can also show that S_{aarr} is the only one of these four-point functions that contributes at leading order. Therefore

$$S_{1122} = 2\,f_F(p^0 + k^0)[1 - f_F(p^0)]\,{\rm Re}\,S_{aarr} \tag{59}$$

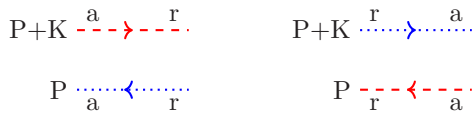

FIG. 10. The pairs of propagators that give pinching poles.

in thermal equilibrium.

We will now evaluate S_{1122} generally without using the KMS condition. Our derivation is thus also valid in nonequilibrium systems. It only relies on the power counting scheme. We know that all gluon rungs must be rr propagators to get the $1/g$ enhancement from the density of soft gluons. Each vertex contains an odd number of a indices so one quark propagator ends with a and one with r at each vertex, see Fig. 9. Finally aa propagators vanish.

We first consider quark rails as in Fig. 8. For the convenience of the reader we draw S_{ar} with red, dashed lines, S_{ra} with blue, dotted lines and S_{rr} with black lines. The first propagator in a quark rail that starts with a must be S_{ar}. The next propagator must then start with a and so on. Thus all propagators are S_{ar} at leading order. Similarly all propagators in a quark rail that starts with r and ends with a are S_{ra}. Finally, quark rails that start and end with a vanish. This means that we can ignore S_{araa}, S_{aara}, S_{arra}, S_{raar}, S_{aaar}, S_{raaa}, and S_{aaaa} at leading order. (In fact, S_{aaaa} vanishes at all orders [39]).

There are more possibilities for quark rails that start and end with r. It is easy to see that they consist of arbitrarily many S_{ra}, then one S_{rr}, and finally arbitrarily many S_{ar}. Thus there are n possibilities for a quark rail with n propagators, which differ in the placement of S_{rr}. See Fig. 8 for the case of three propagators.

The remaining four-point functions can only contribute at leading order if we get pinching poles from each pair of propagators between adjacent gluon rungs. Just like in Eq. (28) that means that one propagator is S_{ra} and the other one S_{ar}, see Fig. 10. This immediately tells us that S_{rara} and S_{arar} can be discarded because they have no pinching poles, see Fig. 11.

We can now express the remaining seven four-point functions in terms of S_{aarr} and S_{rraa}. They all include an rr propagator the pole structure of which can be seen from

$$S_{rr} = \left[\tfrac{1}{2} - F(P)\right](S_{ra} - S_{ar}). \tag{60}$$

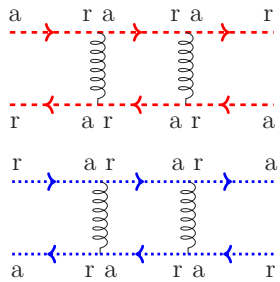

FIG. 11. S_{rara} and S_{arar}. These diagrams do not contribute at leading order because there are no pinching poles.

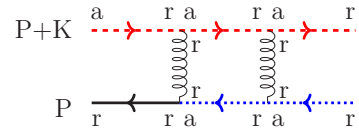

FIG. 12. The only way of placing r/a indices in S_{rarr} at leading order. In a general diagram with arbitrarily many gluon rungs S_{rr} must still be on the far left.

It has poles on both sides of the real axis. At leading order we can drop the term that does not give a pinching pole. As an example we must place the indices in S_{rarr} as in Fig. 12 to get pinching poles from all pairs. Then S_{rr} is on the far left and only the term with S_{ra} contributes. Thus

$$S_{rarr} = \left(\tfrac{1}{2} - F(P)\right)S_{aarr}, \tag{61}$$

where the leading-order diagram for S_{aarr} is in Fig. 13. Similarly, one sees that

$$S_{rrar} = -\left(\tfrac{1}{2} - F(P)\right)S_{rraa} \tag{62}$$

$$S_{arrr} = -\left(\tfrac{1}{2} - F(P+K)\right)S_{aarr} \tag{63}$$

$$S_{rrra} = \left(\tfrac{1}{2} - F(P+K)\right)S_{rraa}. \tag{64}$$

To finish our derivation, we analyze S_{rrrr}, which is more complicated. Each quark rail has one rr propagator. The two S_{rr} must be on top of each other or immediately diagonal to each other since otherwise we will miss a pinching pole pair, see Fig. 14. Let us consider the case of two gluon rungs. In Fig. 15 we analyze the three possibilities of having the rr on top of each other. The remaining possibilities are analyzed in Fig. 16. When these contributions are summed over, all terms cancel except for those corresponding to S_{aarr} and S_{rraa}, see Fig. 17. A similar cancellation takes place for any number of gluon rungs. Specifically, four-point functions with S_{rr} immediately diagonal to each other cancel out with four-point functions with S_{rr} on top of each other. We are then left with

$$S_{rrrr} = -\left(\tfrac{1}{2} - F(P)\right)\left(\tfrac{1}{2} - F(P+K)\right)[S_{rraa} + S_{aarr}]. \tag{65}$$

We have evaluated all terms in Eq. (57) at leading order. Summing up Eqs. (61)–(65) we get that

$$S_{1122} = F(P+K)[1 - F(P)][S_{rraa} + S_{aarr}]. \tag{66}$$

This can be rewritten using $S_{rraa} = S^*_{aarr}$, which can be seen from the definition of the four-point functions or from $S^*_{ra} = -S_{ar}$. We have thus shown that

$$S_{1122} = 2F(P+K)[1 - F(P)]\mathrm{Re}\, S_{aarr} \tag{67}$$

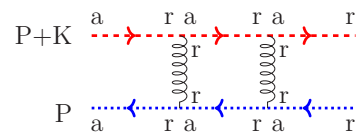

FIG. 13. The only way of placing r/a indices in S_{aarr} at leading order.

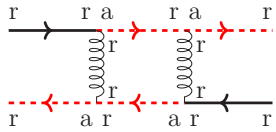

FIG. 14. An example of a diagram that does not contribute to S_{rrrr} at leading order because the propagators in the middle do not give pinching poles.

without using the KMS condition. This expression is convenient because S_{aarr} has a very simple structure, see Fig. 18. In thermal equilibrium F from Eq. (55) reduces to the Fermi-Dirac distribution and we retrieve the equilibrium result, Eq. (59).

The factors of F in Eq. (67) give the momentum distribution of incoming and outgoing quarks including Pauli blocking. Our analysis is valid for on-shell photons, $k^0 \approx k$. The momentum regime where $p^0 > 0$ represents bremsstrahlung off a quark with initial momentum $\mathbf{k}+\mathbf{p}$. The distribution functions are $f_q(\mathbf{k}+\mathbf{p})[1-f_q(\mathbf{p})]$ as expected because there is one incoming and one outgoing quark. Bremsstrahlung off an antiquark is given by $p^0 < -k$. The antiquark's initial momentum in the photon's direction is $-p^0$ and the final momentum is $-(k+p^0)$. The distribution functions are then $[1-f_{\bar{q}}(-\mathbf{k}-\mathbf{p})]f_{\bar{q}}(-\mathbf{p})$. The antiquark distributions are evaluated at negative momentum because we defined the momentum to flow in the direction of quarks. Finally the momentum regime $-k < p^0 < 0$ corresponds to the pair annihilation of a quark with momentum $k+p^0$ and an antiquark with momentum $-p^0$. The distribution functions are $f_q(\mathbf{k}+\mathbf{p})f_{\bar{q}}(-\mathbf{p})$.

B. Summing ladder diagrams

The only remaining task is to sum up the ladder diagrams contributing to S_{aarr}. This gives an integral equation, which describes the LPM effect. We will outline the derivation briefly as it is quite similar to the one in thermal equilibrium, see Refs. [20,40] for further details. The notation follows that of Ref. [41]. The contributing diagrams are shown in Fig. 19 and the procedure for summing them up is in Figs. 20 and 21. One gets an integral equation for the resummed vertex $\mathcal{D}(P,P+K)$, which can be written schematically as

$$\mathcal{D}^\mu = \mathcal{I}^\mu + \int \frac{d^4Q}{(2\pi)^4}\,\mathcal{M}\mathcal{F}\mathcal{D}^\mu. \tag{68}$$

Here $\mathcal{I}^\mu$ is the bare vertex, $\mathcal{F}(P,P+K)$ are quark propagators that give pinching poles and $\mathcal{M}(P,P+K)$ is the contribution from a gluon ladder. The gluon momentum Q is soft, K is the photon momentum and P is the momentum in one of the quark rails. We need to evaluate $\mathcal{F}$ and $\mathcal{M}$.

We let the photon propagate in the z direction. The collinear momentum of the quark momentum is hard, $p^z \sim T$, but the orthogonal components are soft, $\mathbf{p}_\perp \sim gT$. Furthermore the

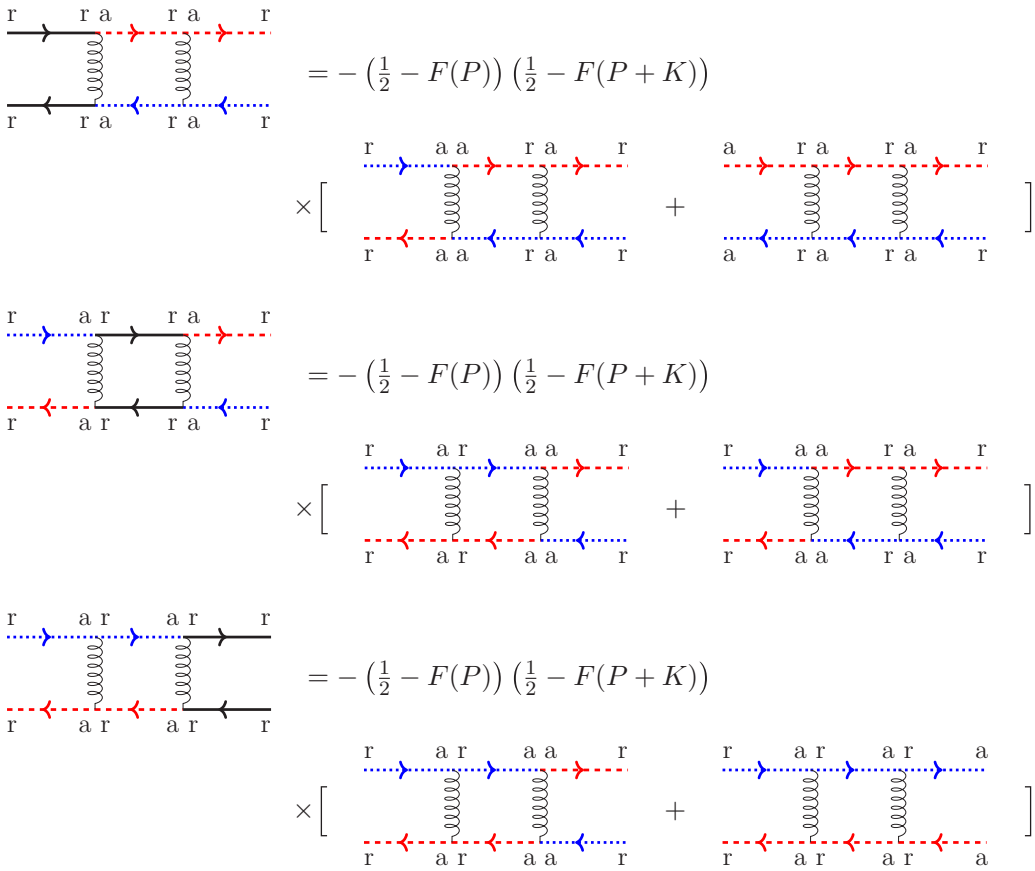

FIG. 15. Leading-order contributions to S_{rrrr} where the S_{rr} propagators are on top of each other.

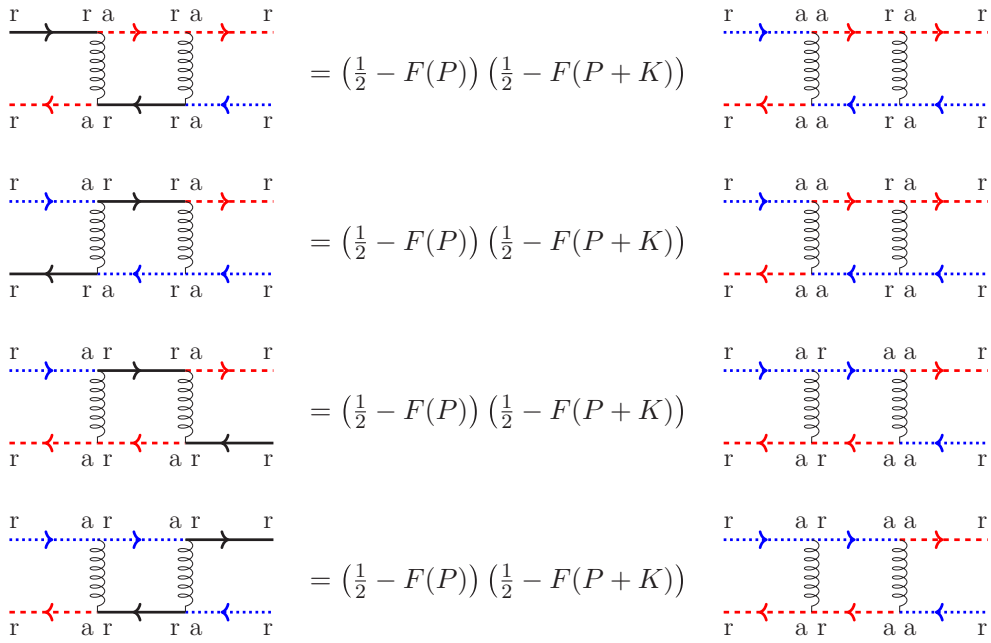

FIG. 16. Leading-order contributions to S_{rrrr} where the S_{rr} propagators are immediately diagonal to each other.

quark is nearly on shell, $p^0 = p^z + O(g^2T)$. It is convenient to decompose the quark propagator in Eq. (51) by helicity,

$$S_{\text{ret}} = \begin{bmatrix} 0 & S^L_{\text{ret}} \\ S^R_{\text{ret}} & 0 \end{bmatrix}. \tag{69}$$

We will focus on the right-handed part. At leading-order one can write it as

$$S^R_{\text{ret}}(P) = \frac{i}{2p}\left[\frac{vv^\dagger}{p^0 + E_{\mathbf{p}} + i\Gamma/2} + \frac{uu^\dagger}{p^0 - E_{\mathbf{p}} + i\Gamma/2}\right], \tag{70}$$

where $E_{\mathbf{p}} = \sqrt{p^2 + m_\infty^2}$ is the quasiparticle energy. This equation has the same form as in equilibrium but the thermal mass m_∞^2 and the decay width Γ are now out-of-equilibrium constants. We have defined $u(\mathbf{p})$ and $v(\mathbf{p})$ to be the eigenvectors of $\boldsymbol{\sigma}\cdot\hat{\mathbf{p}}$ with positive and negative eigenvalues. Their normalization is $v^\dagger v = u^\dagger u = 2p$ and they obey $vv^\dagger = p - \boldsymbol{\sigma}\cdot\mathbf{p}$ and $uu^\dagger = p + \boldsymbol{\sigma}\cdot\mathbf{p}$. The first term in Eq. (70), which has $\text{Re}\, p^0 < 0$ at the pole, describes a left-handed antiquark while the second term describes a right-handed quark.

For simplicity we consider the case when $p^0 > 0$ so only the second term in Eq. (70) contributes. At each gluon vertex we get a factor

$$u^\dagger(\mathbf{p})\,\sigma^\mu\,u(\mathbf{p}) = 2\,(p,\mathbf{p}) \approx 2P^\mu, \tag{71}$$

where the spin indices u come from the adjacent propagators. The gluon rungs then give

$$\begin{aligned}\mathcal{M} &= -4g^2C_F\,P_\mu(K_\nu + P_\nu)\,G^{\mu\nu}_{rr}(Q) \\ &\approx -4g^2C_F\,p^z(k+p^z)\,\hat{K}_\mu\hat{K}_\nu\,\text{Re}\,G^{\mu\nu}_{rr}(Q).\end{aligned} \tag{72}$$

The loop momentum P^μ is nearly collinear with the photon momentum K^μ so only the real and symmetric part of G_{rr} contributes. Here $\hat{K}^\mu = (1,0,0,1)$.

Using $S^R_{\text{adv}} = -S^{R\,*}_{\text{ret}}$ the pinching pole contribution is easily evaluated to be

$$\begin{aligned}\int\frac{dp^0}{2\pi}\mathcal{F}(P;K) &= \int\frac{dp^0}{2\pi}S^R_{\text{adv}}(K+P)S^R_{\text{ret}}(P) \\ &= \frac{1}{4p^z(p^z+k)[\Gamma + i\delta E]},\end{aligned} \tag{73}$$

where

$$\delta E = k^0 + E_{\mathbf{p}}\,\text{sgn}(p^z) - E_{\mathbf{p}+\mathbf{k}}\,\text{sgn}(p^z+k) \tag{74}$$

is of order g^2. When $p^0 < 0$ one gets similar expressions.

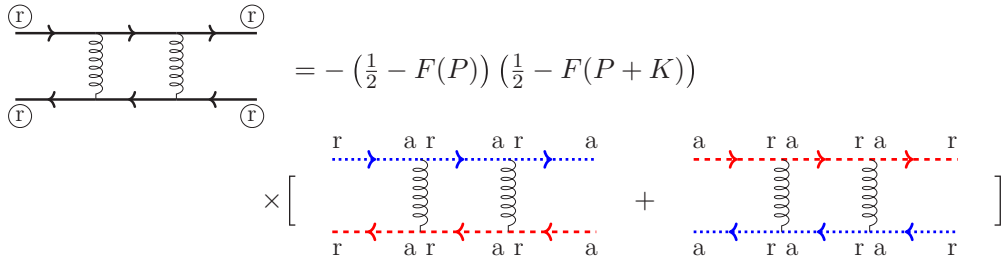

FIG. 17. All leading-order contributions to S_{rrrr} after cancellation.

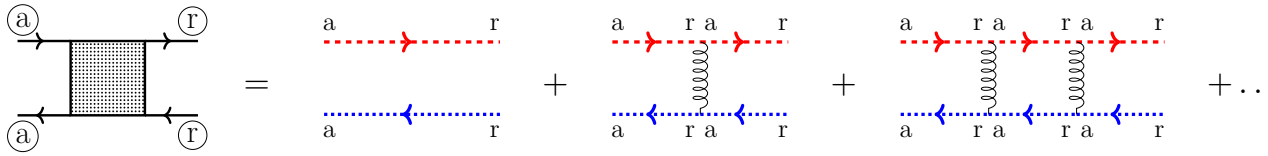

FIG. 18. Leading-order diagrams contributing to S_{aarr}.

We can now assemble all the pieces in Eq. (68). The quark decay width, Eq. (48), can be written as

$$\Gamma = \int \frac{d^2q_\perp}{(2\pi)^2} \mathcal{C}(\mathbf{q}_\perp) \tag{75}$$

with

$$\mathcal{C}(\mathbf{q}_\perp) = g^2 C_F \int \frac{dq_0 dq_z}{(2\pi)^2}\, 2\pi\delta(q_0 - q_z)\, \mathrm{Re}\, G_{rr}(Q)^{\mu\nu} \hat{K}_\mu \hat{K}_\nu. \tag{76}$$

This collision kernel also describes the gluon rungs. Defining

$$\widetilde{f}^\mu(\mathbf{p}) = -4p^z(p^z + k) \int \frac{dp^0}{2\pi} \mathcal{F}\mathcal{D}^\mu, \tag{77}$$

one gets that

$$\sigma^\mu = i\delta E\, \widetilde{f}^\mu(\mathbf{p}) + \int \frac{d^2q_\perp}{(2\pi)^2}\, \mathcal{C}(\mathbf{q}_\perp)[\widetilde{f}^\mu(\mathbf{p}) - \widetilde{f}^\mu(\mathbf{p} + \mathbf{q}_\perp)]. \tag{78}$$

The production rate of photons with momentum $\mathbf{k}$ is

$$k\frac{dR}{d^3k} = \frac{3Q^2\alpha_{EM}}{4\pi^2} \int \frac{d^3p}{(2\pi)^3} F(P + K)[1 - F(P)] \times \frac{p^{z\,2} + (p^z + k)^2}{2p^{z\,2}(p^z + k)^2}\, \mathbf{p}_\perp \cdot \mathrm{Re}\, \mathbf{f}(\mathbf{p}; \mathbf{k}) \tag{79}$$

as can be seen by using Eq. (67), Eq. (79), and evaluating the trace of the quark loop. Here $\mathbf{f}$ is the transverse part of $\widetilde{f}$ without the Pauli matrix. The new factors in p^z and k come from summing over the physical polarization of the photon [20]. Furthermore Q is defined by

$$Q^2 e^2 = \sum_{\text{flavour}} q^2, \tag{80}$$

where we sum over the different flavors of light quarks. As explained above, F is the momentum distribution of quarks including Fermi suppression for outgoing quarks,

$$F(P) = f_q(\mathbf{p})\theta(p^0) + [1 - f_{\bar{q}}(-\mathbf{p})]\theta(-p^0). \tag{81}$$

Finally $p^0 = (-k^0 + E_{\mathbf{p}}\, \mathrm{sgn}(p^z) + E_{\mathbf{p}+\mathbf{k}}\, \mathrm{sgn}(p^z + k))/2$.

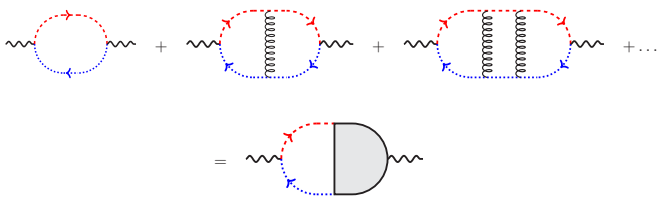

FIG. 19. The LPM diagrams that contribute at leading order to the photon polarization tensor Π^γ_{12}. Red propagators are S_{ar} and blue propagators are S_{ra}.

In this expression $\mathbf{f}$ satisfies a Boltzmann-like integral equation

$$\mathbf{p}_\perp = i\delta E\, \mathbf{f}(\mathbf{p}_\perp) + \int \frac{d^2q_\perp}{(2\pi)^2}\, \mathcal{C}(\mathbf{q}_\perp)[\mathbf{f}(\mathbf{p}_\perp) - \mathbf{f}(\mathbf{p}_\perp + \mathbf{q}_\perp)]. \tag{82}$$

Here $\mathbf{f}(\mathbf{p}_\perp;\ p^z, \mathbf{k})$ is an analog of the density of hard quarks with transverse momentum $\mathbf{p}_\perp$ that emit a photon with momentum $\mathbf{k}$. The term $i\delta E\, \mathbf{f}$ works like a time derivative in momentum space. The integral describes the change in transverse momentum of the quarks through the exchange of soft gluons with the medium. The gain term comes from the gluon rungs while the loss term comes from the quark decay width. Equations (26) and (82) agree with the Abelian limit of the results of Ref. [23] where a kinetic theory of quarks and gluons was used to study the LPM effect in a perhaps more heuristic way.

In an isotropic plasma, $f(\mathbf{p}) = f(p)$, one gets a simple expression for the collision kernel $\mathcal{C}(\mathbf{q}_\perp)$ by using a sum rule [23,42]. This special case is relevant for the bulk viscous correction to photon production. Specifically,

$$\mathcal{C}(\mathbf{q}_\perp) = g^2 C_F\, \Omega\left[\frac{1}{\mathbf{q}_\perp^2} - \frac{1}{\mathbf{q}_\perp^2 + m_D^2}\right]. \tag{83}$$

Here

$$\Omega = \frac{\int_0^\infty dp\, p^2\, [2N_f f_q(1 - f_q) + 2N_c f_g(1 + f_g)]}{-\int_0^\infty dp\, p^2\, \frac{d}{dp}[2N_f f_q + 2N_c f_g]} \tag{84}$$

characterizes the occupation density of soft gluons. Furthermore,

$$m_D^2 = \frac{g^2}{\pi^2} \int_0^\infty dp\ p[2N_f f_q(p) + 2N_c f_g(p)] \tag{85}$$

is a nonequilibrium Debye mass. In the isotropic case the LPM effect only depends on Ω, m_D^2, and m_∞^2, the nonequilibrium mass of hard quarks, along with the momentum distribution F from Eq. (81).

In an anisotropic plasma the collision kernel in Eq. (76) and the quark decay width in Eq. (75) are divergent, because of the gauge field instabilities discussed previously. For the moment, the simplest solution is to impose that the anisotropy is small enough for the divergences to be subleading in the coupling. At leading order only $g^2 T \lesssim Q \lesssim gT$ contributes to the kernel

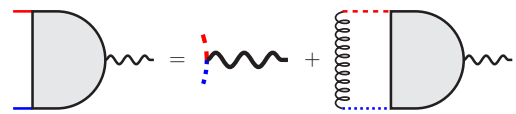

FIG. 20. Procedure for summing up the diagrams in Fig. 19.

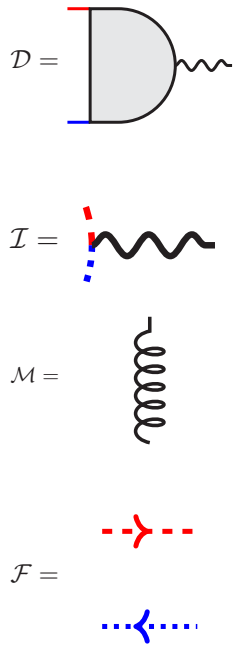

FIG. 21. Definition of the quantities in Eq. (68).

so one demands that the divergence takes place at the ultrasoft scale of $Q \lesssim g^2 T$. For the momentum distribution in Eq. (9) this leads to $|\xi| \lesssim g^2$. We illustrate this with the α collective mode of Ref. [30]. In that case, the divergence in the quark decay width comes from terms such as

$$\int_{g^2T}^{gT} d^4Q\; G_{\rm ret} G_{\rm adv} \sim \int_{g^2T}^{gT} \frac{d^4Q}{\left(\mathbf{q}^2 + m_\alpha^2\right)^2 + \left(\frac{\pi q^0}{4q} m_D^2\right)^2}, \quad (86)$$

where $G_{\rm adv} = G_{\rm ret}^*$ and we have taken the limit $q^0 \to 0$ where possible. At leading order in ξ, the static limit of the α self-energy component is [30]

$$m_\alpha^2 = -\frac{\xi}{6}(1 + \cos 2\theta_n) m_D^2. \quad (87)$$

It depends on the angle between the gluon momentum and the direction of the anisotropy, θ_n. For $\xi > 0$, m_α^2 is negative, which leads to divergences. Clearly, the divergence is at $q \lesssim g^2 T$ if $\xi \lesssim g^2$.

VI. CONCLUSION

The quark-gluon plasma created in heavy-ion collisions deviates from local thermal equilibrium. To understand how the plasma radiates photons one needs to include the effects of these deviations. This means analyzing photon production in a nonequilibrium plasma. Understanding the effect of viscosity on photons could in turn be used to extract the transport coefficients of QGP from photonic observables.

In this paper we have studied photon production through bremsstrahlung and pair annihilation in a nonequilibrium QGP. Using field theory, we derived integral equations describing these channels and the LPM effect: Eqs. (82) and (76). Along the way, we showed that the resummed rr propagator of gluons in an anisotropic plasma has an imaginary part that does not contribute at leading order but could be important at higher order. We also derived a simple expression for the rr propagator of hard, on-shell quarks. Finally, we presented a way of summing up ladder diagrams without using the KMS condition, which is only true in thermal equilibrium. Our derivation of the integral equation is valid for low anisotropy. In the special case of an isotropic plasma the integral equation only depends on three nonequilibrium constants.

To solve the integral equation one needs to assume some momentum distribution $f(\mathbf{p})$. Work is ongoing on evaluating the bulk and shear viscous corrections to photon production using $f(\mathbf{p})$ derived from kinetic theory. In the future, these ideas could be used to analyze jets in a nonequilibrium plasma and to extend this work to higher anisotropy. This might allow for the extraction of transport coefficients of QGP from jet observables.

ACKNOWLEDGMENTS

We thank Stanisław Mrówczyński for useful discussions. This work was supported in part by the Natural Sciences and Engineering Research Council of Canada. S.H. acknowledges a scholarship from the Department of Physics of McGill University, and C.G. acknowledges support from the Canada Council for the Arts through its Killam Research Fellowship program.

[1] B. V. Jacak and B. Muller, The exploration of hot nuclear matter, Science **337**, 310 (2012).
[2] C. Gale, S. Jeon, and B. Schenke, Hydrodynamic modeling of heavy-ion collisions, Int. J. Mod. Phys. A **28**, 1340011 (2013).
[3] U. Heinz and R. Snellings, Collective flow and viscosity in relativistic heavy-ion collisions, Ann. Rev. Nucl. Part. Sci. **63**, 123 (2013).
[4] G. Vujanovic, C. Young, B. Schenke, R. Rapp, S. Jeon, and C. Gale, Dilepton emission in high-energy heavy-ion collisions with viscous hydrodynamics, Phys. Rev. C **89**, 034904 (2014).
[5] J.-F. Paquet, C. Shen, G. S. Denicol, M. Luzum, B. Schenke, S. Jeon, and C. Gale, Production of photons in relativistic heavy-ion collisions, Phys. Rev. C **93**, 044906 (2016).
[6] R. Baier, H. Nakkagawa, A. Niegawa, and K. Redlich, Production rate of hard thermal photons and screening of quark mass singularity, Z. Phys. C **53**, 433 (1992).
[7] J. I. Kapusta, P. Lichard, and D. Seibert, High-energy photons from quark-gluon plasma versus hot hadronic gas, Phys. Rev. D **44**, 2774 (1991); Erratum: High-energy photons from quark-gluon plasma versus hot hadronic gas, **47**, 4171 (1993).

[8] M. Strickland, Thermal photons and dileptons from nonequilibrium quark-gluon plasma, Phys. Lett. B **331**, 245 (1994).
[9] R. Baier, M. Dirks, K. Redlich, and D. Schiff, Thermal photon production rate from nonequilibrium quantum field theory, Phys. Rev. D **56**, 2548 (1997).
[10] F. Gelis, H. Niemi, P. V. Ruuskanen, and S. S. Räsänen, Photon production from nonequilibrium QGP in heavy ion collisions, *Ultra-relativistic nucleus-nucleus collisions. Proceedings of the 17th International Conference, Quark Matter 2004, Oakland, USA, January 11–17, 2004*, J. Phys. G **30**, S1031 (2004).
[11] B. Schenke and M. Strickland, Photon production from an anisotropic quark-gluon plasma, Phys. Rev. D **76**, 025023 (2007).
[12] M. Dion, J.-F. Paquet, B. Schenke, C. Young, S. Jeon, and C. Gale, Viscous photons in relativistic heavy ion collisions, Phys. Rev. C **84**, 064901 (2011).
[13] C. Shen, J.-F. Paquet, U. Heinz, and C. Gale, Photon emission from a momentum anisotropic quark-gluon plasma, Phys. Rev. C **91**, 014908 (2015).
[14] S. Hauksson, C. Shen, S. Jeon, and C. Gale, Bulk viscous corrections to photon production in the quark-gluon plasma, Nucl. Part. Phys. Proc. **289**, 169 (2017).
[15] P. Aurenche, F. Gelis, and H. Zaraket, Landau-Pomeranchuk-Migdal effect in thermal field theory, Phys. Rev. D **62**, 096012 (2000).
[16] L. D. Landau and I. Pomeranchuk, Limits of applicability of the theory of bremsstrahlung electrons and pair production at high-energies, Dokl. Akad. Nauk Ser. Fiz. **92**, 535 (1953).
[17] L. D. Landau and I. Pomeranchuk, Electron cascade process at very high-energies, Dokl. Akad. Nauk Ser. Fiz. **92**, 735 (1953).
[18] A. B. Migdal, Quantum kinetic equation for multiple scattering, Dokl. Akad. Nauk Ser. Fiz. **105**, 77 (1955).
[19] A. B. Migdal, Bremsstrahlung and pair production in condensed media at high-energies, Phys. Rev. **103**, 1811 (1956).
[20] P. Arnold, G. D. Moore, and L. G. Yaffe, Photon emission from ultrarelativistic plasmas, J. High Energ. Phys. 11 (2001) 057.
[21] P. Arnold, G. D. Moore, and L. G. Yaffe, Photon emission from quark gluon plasma: Complete leading order results, J. High Energ. Phys. 12 (2001) 009.
[22] R. Kubo, Statistical mechanical theory of irreversible processes. 1. General theory and simple applications in magnetic and conduction problems, J. Phys. Soc. Jpn. **12**, 570 (1957); P. C. Martin and J. S. Schwinger, Theory of many particle systems. 1, Phys. Rev. **115**, 1342 (1959).
[23] P. B. Arnold, G. D. Moore, and L. G. Yaffe, Effective kinetic theory for high temperature gauge theories, J. High Energ. Phys. 01 (2003) 030.
[24] M. Le Bellac, *Thermal Field Theory* (Cambridge University Press, Cambridge, 2011).
[25] K.-C. Chou, Z.-B. Su, B.-L. Hao, and L. Yu, Equilibrium and nonequilibrium formalisms made unified, Phys. Rept. **118**, 1 (1985).
[26] L. V. Keldysh, Diagram technique for nonequilibrium processes, Zh. Eksp. Teor. Fiz. **47**, 1515 (1964) [Sov. Phys. JETP **20**, 1018 (1965)].
[27] S. Mrowczynski and U. W. Heinz, Towards a relativistic transport theory of nuclear matter, Ann. Phys. (NY) **229**, 1 (1994).
[28] E. Calzetta and B. L. Hu, Nonequilibrium Quantum Fields: Closed Time Path Effective Action, Wigner Function and Boltzmann Equation, Phys. Rev. D **37**, 2878 (1988).
[29] J. Berges, Introduction to nonequilibrium quantum field theory, in *Proceedings of the 9th Hadron Physics and 7th Relativistic Aspects of Nuclear Physics (HADRON-RANP 2004): A Joint Meeting on QCD and QGP: Rio de Janeiro, Brazil, March 28–April 3, 2004*, edited by M. Bracco, M. Chiapparini, E. Ferreira, and T. Kodama, AIP Conf. Proc. No. 739 (AIP, New York, 2005), p. 3.
[30] P. Romatschke and M. Strickland, Collective modes of an anisotropic quark gluon plasma, Phys. Rev. D **68**, 036004 (2003).
[31] S. Mrowczynski, B. Schenke, and M. Strickland, Color instabilities in the quarkgluon plasma, Phys. Rept. **682**, 1 (2017).
[32] C. Greiner and S. Leupold, Interpretation and resolution of pinch singularities in nonequilibrium quantum field theory, Eur. Phys. J. C **8**, 517 (1999).
[33] J. Serreau, Out-of-equilibrium electromagnetic radiation, J. High Energ. Phys. 05 (2004) 078.
[34] P. Aurenche, F. Gelis, H. Zaraket, and R. Kobes, Bremsstrahlung and photon production in thermal QCD, Phys. Rev. D **58**, 085003 (1998).
[35] S. Mrowczynski and M. H. Thoma, Hard loop approach to anisotropic systems, Phys. Rev. D **62**, 036011 (2000).
[36] M. Nopoush, Y. Guo, and M. Strickland, The static hard-loop gluon propagator to all orders in anisotropy, J. High Energ. Phys. 09 (2017) 063.
[37] J. I. Kapusta and C. Gale, *Finite-Temperature Field Theory: Principles and Applications* (Cambridge University Press, Cambridge, 2011).
[38] P. B. Pal, Representation-independent manipulations with Dirac matrices and spinors, arXiv:physics/0703214 [physics.ed-ph].
[39] E. Wang and U. W. Heinz, A Generalized fluctuation dissipation theorem for nonlinear response functions, Phys. Rev. D **66**, 025008 (2002).
[40] K. A. Mamo and H.-U. Yee, Spin polarized photons from an axially charged plasma at weak coupling: Complete leading order, Phys. Rev. D **93**, 065053 (2016).
[41] S. Jeon, Hydrodynamic transport coefficients in relativistic scalar field theory, Phys. Rev. D **52**, 3591 (1995).
[42] P. Aurenche, F. Gelis, and H. Zaraket, A Simple sum rule for the thermal gluon spectral function and applications, J. High Energ. Phys. 05 (2002) 043.